

Generating Likely Counterfactuals Using Sum-Product Networks

Jiří Němeček, Tomáš Pevný & Jakub Mareček

September 24, 2024

Abstract

Explainability of decisions made by AI systems is driven by both recent regulation and user demand. These decisions are often explainable only *post hoc*, after the fact. In counterfactual explanations, one may ask what constitutes the best counterfactual explanation. Clearly, multiple criteria must be taken into account, although “distance from the sample” is a key criterion. Recent methods that consider the plausibility of a counterfactual seem to sacrifice this original objective. Here, we present a system that provides high-likelihood explanations that are, at the same time, close and sparse. We show that the search for the most likely explanations satisfying many common desiderata for counterfactual explanations can be modeled using mixed-integer optimization (MIO). In the process, we propose an MIO formulation of a Sum-Product Network (SPN) and use the SPN to estimate the likelihood of a counterfactual, which can be of independent interest.

1 Introduction

There is no doubt that the use of artificial intelligence (AI) is increasing. Consequently, a better understanding of the AI models deployed is needed, especially in high-risk scenarios [14]. Understanding AI models is usually seen through the lens of trustworthy and explainable AI (XAI), which is concerned with techniques that help people understand, manage, and improve trust in AI models [21, 7, 5]. Explanations also serve an important role in debugging models to ensure that they do not rely on spurious correlations and traces of processing correlated with labels, such as timestamps.

In a *post-hoc* explanation, a vendor of an AI system provides an individual user with a personalized explanation of an individual decision made by the AI system, improving the model’s trustworthiness [30, 33]. In this context, personalized explanations are often called local explanations because they explain the model’s decision locally, around a given sample, such as one person’s input. Thus, local explanations provide information relevant to the user without revealing global information about the model, regardless of whether the model is interpretable *a priori*. Consider, for example, credit decision-making in financial services. The models utilized need to be interpretable *a priori*, cf. Equal Credit Opportunity Act in the US [15] and related regulation [16, 17]

in the European Union, but an individual who is denied credit may still be interested in a personalized, local explanation.

A well-known example of local explanations is the counterfactual explanation (CE). CE answers the question “How should a sample be changed to obtain a different result?” [47]. In the example of credit decision-making, a denied client might ask what they should do to obtain the loan. The answer would take the form of a CE. For example, “Had you asked for half the amount of credit, your application would have been accepted”. As illustrated, CE can be easily understood [9, 20]. However, their usefulness is influenced by many factors [20], including validity, similarity, sparsity, diversity, actionability, causality, and plausibility.

Here, we focus on the plausibility of counterfactual explanations. In the above example, halving the credit amount might not be plausible because the purpose of the credit application might require a higher amount. A closer CE with similar plausibility might be of greater use to the client. At the same time, plausibility does not have a clear definition. The definition of Guidotti suggests CE not being an outlier and measures it as the mean distance to data [20]. A Local Outlier Factor is often used [e.g., 29]. Alternatively, Jiang et al. define a “plausible region” as a convex hull of k nearest neighbors of the factual [27]. Another approach to the plausibility of CE uses (Conditional) Variational Auto Encoders [28, 41, 20] in likelihood estimation. However, variational auto-encoders provide only a lower bound on likelihood and are intractable models of probability distributions [28, 32], which means that one cannot efficiently compute the exact likelihood or marginalize variables with polynomial-time complexity with respect to the size of the encoder [11]. We, therefore, investigate how to maximize the likelihood when generating CE explanations.

Our Contribution We propose a method for Likely Counterfactual Explanations (LiCE) using Sum-Product Networks (SPN) [43] to estimate the likelihood of a counterfactual, thus plausibility, while satisfying most other common desiderata modeled within mixed-integer optimization (MIO), see Table 1 for comparison to existing methods.

MIO has been used to search for CEs before the term CE was first used [13]. MIO has the favorable properties of being model-agnostic (as long as the model can be formulated in MIO) and satisfying validity by design. Russell [45] considered generating multiple explanations using a custom MIO solver. One can also implement various constraints [e.g. 34]. At the same time, this improves upon the early uses of tractable probabilistic models in CE generation, such as [1], which estimate a Gaussian Mixture Model and which we refer to as PlaCE (Plausible CEs), where PlaCE is limited in its inability to handle categorical features and non-linear classifiers.

The advantage can be illustrated on the German Credit dataset [23]. See Figure 1, where CEs produced by a number of methods considering the diversity or plausibility of CE are compared against the factual (white cross) in the plane, where the horizontal axis represents the amount of credit and where the vertical axis is the duration. The heatmap corresponds to the likelihood of the CE, evaluated using an SPN trained on the randomly split training set (80% of the dataset). For example, C-CHVAE [41] and FACE [44] suggest approximately halving the credit amount. The most plausible ex-

Table 1: *Method comparison.* A check mark indicates that a given method claims to possess the given feature. The star symbol (*) means that the method is model-agnostic as long as the classifier can be expressed using MIO. Complex data means data with continuous, categorical, ordinal, and discrete contiguous values. Exogenous property holds if a method can generate unseen data samples as CEs.

	LiCE	PROPLACE [27]	C-CHVAE [41]	FACE [44]	DiCE [38]	PlaCE [1]	DACE [29]
Causality	✓						
Sparsity	✓				✓	✓	
Plausibility	✓	✓	✓	✓		✓	✓
Model-agnostic	✓*		✓	✓			✓*
Complex data	✓			✓			
Exogenous	✓	✓	✓		✓	✓	✓

planation produced by DiCE [38] suggests decreasing the credit amount by almost a third while reducing the Duration to a single year. VAE and PROPLACE [27] suggest decreasing the credit amount even further to below 3000. In contrast, MIO finds a counterfactual with the sought credit amount and suggests decreasing the Duration by two months. Because the visualization is a 2-dimensional projection, some changes are not visualized. LiCE, however, changes only one “hidden” feature (Installment rate as a percentage of disposable income). To compare, all other methods change at least six features (except MIO, which changes two), showing poor sparsity.

In particular, we propose:

- Sum-Product Network encoded into an MIO formulation.
- Sum-Product Network as a measure of plausibility of CE, which allows the integration of the condition directly into the MIO formulation.
- LiCE method for the generation of CEs. An MIO model that can be constrained by or optimized with respect to the most common desiderata regarding CE generation.

Notation used Throughout the paper, we consider a classification problem where the dataset \mathcal{D} is a set of 2-tuples $(\mathbf{x}, y) \in \mathcal{D}$. Each input vector $\mathbf{x} \in \mathcal{X} \subseteq \mathbb{R}^P$ consists of P features and is taken from the input space \mathcal{X} that can be smaller than P -dimensional real space (e.g., can contain categorical values). x_j is the value of the j -th feature of the sample \mathbf{x} . We have C classes and describe the set of classes $[C] = \{1, \dots, C\}$. $y \in [C]$ is the true class of the sample \mathbf{x} . Finally, we have a classifier $h(\mathbf{x}) = \hat{y} \in [C]$ that predicts the class \hat{y} for the sample \mathbf{x} . Our goal is to find a set of M counterfactuals $\mathcal{C}_{\mathbf{x}} = \{\mathbf{x}'_{(1)}, \dots, \mathbf{x}'_{(M)}\}$ for a given \mathbf{x} . Note that the bold \mathbf{x}' means that the subscripts refer to indices of counterfactual instances within $\mathcal{C}_{\mathbf{x}}$ rather than a feature index. More details on the notation are in Appendix A.1.

2 Related Work

There is a plethora of work on the search for CEs, as recently surveyed [20, 7, 5, e.g.]. See [30, cf. Table 1] for a one-page overview. In our overview, we will focus on

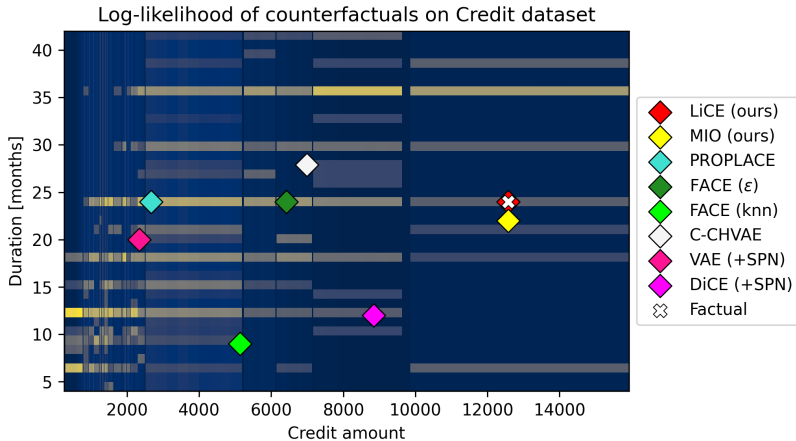


Figure 1: The heatmap shows the marginalized likelihood distribution of the German Credit dataset into a 2-dimensional space of Credit amount and Duration features. The factual (white cross) and CEs are also projected to the two dimensions. The factual is classified as being denied. Most CE methods choose distant points, sometimes with poor likelihood. The proposed method (LiCE) strikes a balance between likelihood and proximity. For methods capable of outputting multiple CEs (DiCE, VAE, MIO, LiCE), we show the most likely out of 10, based on the SPN.

methods that support both categorical and continuous-valued features, with objectives related to the plausibility, actionability, or likelihood of the CE and methods utilizing MIO.

Historically, a number of terms have been used for related approaches. Focusing on approaches that use MIO, pioneering work [13] considered classifiers based on additive tree models and extracted an optimal plan to change a given input to a desired class at a minimum cost, calling the problem “optimal action extraction” (OAE). In parallel, similar approaches have been developed under the banner of “actionable recourse” [46] or “algorithmic recourse” [30, 31]. Developing upon this, [31] distinguish between contrasting explanations and consequential explanations, where actions are modeled explicitly in a causal model. We use the term counterfactual explanations (CEs), popularized by [47, e.g.].

Given the many CE methods that generate various CEs, one must deal with the disagreement problem [6], where a user could be misled by the explainer who selects the CEs that align with their interests. We argue for the use of exact methods (e.g., MIO) that return the same optimal CEs each time.

2.1 Counterfactuals

We define a counterfactual explanation in accordance with previous works as $\mathbf{x}' \in \mathcal{X}$ such that $h(\mathbf{x}) \neq h(\mathbf{x}')$ and the distance between \mathbf{x}' and \mathbf{x} is in some sense minimal [20, 47]. We refer to \mathbf{x} as factual and \mathbf{x}' as counterfactual. As mentioned above, there are many desiderata regarding the properties of CEs. Following [20], the common

desiderata include:

- *Validity*. \mathbf{x}' should be classified differently than \mathbf{x}
- *Similarity*. \mathbf{x}' should be similar (close) to \mathbf{x}
- *Sparsity*. \mathbf{x}' should change only a few features compared to \mathbf{x} , i.e., minimize $\|\mathbf{x}' - \mathbf{x}\|_0$
- *Diversity*. Each $\mathbf{x}'_{(m)} \in \mathcal{C}_{\mathbf{x}}$ should be as different as possible from any other CE in the set, ideally by proposing changes in different features. For example, one CE recommends increasing the income; another one should recommend decreasing the loan amount instead. An important example of a CE library aiming for diversity is DiCE [38]. In MIO, this is usually achieved by adding constraints and resolving the formulation [45, 36].
- *Actionability*. A counterfactual should change only features that can be influenced in reality. It should also change them correctly, such as only increasing the age.
- *Causality*. Given that we know some causal relationships between the features, the generated CEs should follow them. For example, if \mathbf{x}' contains a decrease in the total loan amount, the number of payments or their amount should also decrease.
- *Plausibility*. While computing the probability of a CE in a given probabilistic model may be NP-Hard, CEs should not be outliers in the dataset \mathcal{D} [20, 51]. A natural way to measure normality is using the likelihood of \mathbf{x}' , which can be estimated for example using autoencoders [41, 34, e.g.] (providing just lower bound), by Gaussian Mixture Models [1], or by probabilistic circuits, e.g., Sum-Product Networks (SPNs), used in this paper, and promote CEs with the highest estimated likelihood. The probabilistic models usually scale better than nearest-neighbour based methods like the Local Outlier Factor used in [29].

2.2 Mixed-Integer Optimisation

Mixed-integer optimization (MIO, [49]) is a powerful framework for modeling and solving optimization problems, where some decision variables take values from a discrete set while others are continuously valued. Non-trivially, the problem is in NP [39] and is NP-Hard, in general. There has been fascinating progress in the field in the past half-century [4]. State-of-the-art solvers based on the branch-and-bound-and-cut approach can often find global, certified optima for instances with millions of binary variables within hours, while there are pathological instances on under a thousand variables whose global optima are still unknown. Naturally, MIO is widely used in areas of machine learning, where both discrete and continuous decision variables need to be optimized jointly [e.g., 25].

In counterfactual reasoning, where we often need to consider both categorical and continuous-valued features, MIO has been used since the early days [13, 46, 45, 29,

40, 36, 26, 27]. A crucial advance has been Russell’s mixed polytope formulation [45], which neatly combines categorical and continuous values. A feature j takes a continuous value from the $[L_j, U_j]$ range or one of K_j distinct categorical values. This is useful for modeling data with missing features, especially when there is a description of why the value is missing [45]. To model the mixed polytope [45] of a counterfactual for the feature j , we create a one-hot encoding for K_j discrete values into binary variables $d_{j,k}$ and a continuous variable c_j with a binary indicator variable d_j^{cont} equal to 1 when the feature takes a continuous value. In summary:

$$\sum_{k=1}^{K_j} d_{j,k} + d_j^{\text{cont}} = 1 \quad (1)$$

$$c_j = F_j d_j^{\text{cont}} - l_j + u_j \quad (2)$$

$$0 \leq l_j \leq (F_j - L_j) d_j^{\text{cont}} \quad (3)$$

$$0 \leq u_j \leq (U_j - F_j) d_j^{\text{cont}} \quad (4)$$

$$d_j^{\text{cont}}, d_{j,k} \in \{0, 1\} \quad \forall k \in [K_j], \quad (5)$$

where F_j is either the original value x_j or the median value if the factual x_j has a categorical value instead. The computation of counterfactual c_j in (2) uses two non-negative variables, l_j and u_j , representing the decrease and increase in the continuous value, respectively. This construction facilitates the computation of the absolute difference from the factual. Since we minimize their (weighted) sum, at least one of them will always equal 0. [45]

2.3 Sum-Product Networks

Probabilistic circuits (PCs) [11] are tractable probabilistic models (or rather, computational graphs) that support exact probabilistic inference and marginalization in time linear w.r.t. their representation size. Probabilistic circuits are defined by a tuple $(\mathcal{G}, \psi, \theta)$, where $\mathcal{G} = (\mathcal{V}, \mathcal{E})$ is a Directed Acyclic Graph (DAG) defining the computation model, a scope-function $\psi : \mathcal{V} \rightarrow 2^{[P]}$ defines a subset of features over which the node defines its distribution, and a set of parameters θ . To simplify the notation, we define a function $\text{pred}(n)$, giving a set of children (predecessors) of an inner node n .

An important subclass of PCs are Sum-Product Networks (SPNs), which restrict PCs such that the inner (non-leaf) nodes can be only sums and products. We denote the set of sum nodes \mathcal{V}^Σ and product nodes \mathcal{V}^Π .

Leaf node $n^L \in \mathcal{V}^L = \{n \mid \text{pred}(n) = \emptyset\}$ within SPNs takes a value O_{n^L} from a (tractable) distribution over its scope $\psi(n^L)$ parametrized by θ_{n^L} .

Product node $n^\Pi \in \mathcal{V}^\Pi$ performs a product of probability distributions defined by its children

$$O_{n^\Pi}(\mathbf{x}) = \prod_{a \in \text{pred}(n^\Pi)} O_a(x_{\psi(a)}) \quad (6)$$

. The scope of product nodes must satisfy decomposability, meaning that the scopes of its children are disjoint, i.e., $\bigcap_{a \in \text{pred}(n^\Pi)} \psi(a) = \emptyset$, but complete $\bigcup_{a \in \text{pred}(n^\Pi)} \psi(a) = \psi(n^\Pi)$.

Sum node $n^\Sigma \in \mathcal{V}^\Sigma$ has its value defined as

$$O_{n^\Sigma}(\mathbf{x}) = \sum_{a \in \text{pred}(n^\Sigma)} w_{a,n^\Sigma} \cdot O_a(\mathbf{x}), \quad (7)$$

where weights $w_{a,n^\Sigma} \geq 0$ and $\sum_{a \in \text{pred}(n^\Sigma)} w_{a,n^\Sigma} = 1$. The value of a sum node is thus a mixture of distributions defined by its children. The scope of each sum node must satisfy completeness (smoothness), i.e., it must hold that $\psi(a_1) = \psi(a_2) \forall a_1, a_2 \in \text{pred}(n^\Sigma)$.

The root node n^{root} (a node without parents) has the scope-function over all features, i.e., $\psi(n^{\text{root}}) = [P]$. There are a variety of methods for training SPN [50], out of which we use a variant of LearnSPN [18] with k-means clustering, as implemented in the SPFlow library [37].

3 SPN encoding into MIO

To utilize the computation of likelihood provided by SPNs to ensure plausible counterfactuals generated using MIO, we formulate them using integer linear constraints. Specifically, we propose an MIO formulation for a bounded approximation of an SPN. Since the multiplication of variables in the product nodes is not desirable for linear formulations and numerical stability is an issue for MIO solvers, we perform all computations in the log space.

Leaf nodes Leaves are represented by probability distributions over a single feature. These, especially in the case of histograms, can be expressed as (or approximated by) piece-wise linear functions. The modeling of piece-wise linear within MIO is well-studied [e.g., 24], and various implementations are available out-of-the-box in the Pyomo modeling library [8]. We suggest a possible alternative formulation of a histogram in Appendix A.2.1. We don't need to map categorical values to histograms; we can use the $d_{j,k}$ variables directly by computing a dot product between probability values and the one-hot encoding.

Product nodes Having obtained the output of the leaf nodes, we move to the inner nodes. Each node n produces an output o_n combining the outputs o_a , $a \in \text{pred}(n)$ of its predecessors. Consider now a product node $n \in \mathcal{V}^\Pi$, with output defined as a product of predecessor outputs. Since we consider all computations in log space, this translates to

$$o_n = \sum_{a \in \text{pred}(n)} o_a \quad \forall n \in \mathcal{V}^\Pi. \quad (8)$$

Sum nodes So far, we produced the exact output values. However, this is no longer possible for sum nodes. Sum node $n \in \mathcal{V}^\Sigma$ is defined as a weighted sum of predecessor a outputs. In log space, the sum would translate to $o_n^* = \log \sum_{a \in \text{pred}(n)} w_{a,n} \exp(o_a)$, which we cannot model easily. To approximate it, we notice that $w_{a,n} \exp(o_a) =$

$\exp(o_a + \log w_{a,n})$, and that we can approximate $\log \sum \exp(z)$ by $\max z$. Specifically, let $z_a = o_a + \log w_{a,n}$ and we bound

$$\begin{aligned} \max_{a \in \text{pred}(n)} z_a &= \log \exp\left(\max_{a \in \text{pred}(n)} z_a\right) \\ &\leq \log \sum_{a \in \text{pred}(n)} \exp(z_a) = o_n^* \\ &\leq \log \left(|\text{pred}(n)| \exp\left(\max_{a \in \text{pred}(n)} z_a\right) \right) = \log(|\text{pred}(n)|) + \max_{a \in \text{pred}(n)} z_a. \end{aligned}$$

That is: we can bound the true o_n^* from below, and the error in the estimate will be at most logarithm of the number of predecessors. Putting this into our formulation, we once again utilize the general max constraint, linearized by the solver

$$o_n = \max_{a \in \text{pred}(n)} (o_a + \log w_{a,n}) \quad \forall n \in \mathcal{V}^\Sigma, \quad (9)$$

where o_n is in a conservative estimate of the true o_n^* as explained above. If we wanted to use the overestimation variant, we could easily add $\log |\text{pred}(n)|$ to the estimate o_n . When this approximation of sum nodes by max nodes is used during training, it is called hard EM and was recommended by Poon and Domingos in the original paper introducing the SPN architecture [43]. Using hard EM during training, therefore, would make the approximation exact.

4 Our Method

We now present our model for Likely Counterfactual Explanations (LiCE). Combining the strictness and global properties of MIO with the likelihood modeling capabilities of SPNs, we create a model capable of satisfying most of the common desiderata for CEs. We assume that all continuous values are normalized to the range $[0, 1]$.

Input encoding To encode the input vector, we extend the mixed polytope formulation [45], as explained in Eqs. 1–5 on page 6. The mixed polytope encoding works for purely continuous values by setting $K_j = 0$. For purely categorical features, the original implementation contains an issue. The first categorical value (represented by zero) is mapped to the continuous variable. This seems to work fine for the logarithmic regression [45], but it failed on non-monotone neural networks, leading to non-binary outputs. This was corrected by replacing the continuous variable c_j with another binary decision variable, making it a standard one-hot encoding.

As an input to the neural network, we concatenate all variables c_j and $d_{j,k}$ (but not d_j^{cont}) into a single vector. With some abuse of the notation, we denote this vector \mathbf{x}' . We further use \mathcal{X} for the space of encoded inputs and P for the number of encoded variables when there is no risk of confusion.

Model encoding To encode the classification model, we use the OMLT library [10]. It enables simple encoding of various machine-learning models, including neural networks and gradient-boosted trees. In our experiments, we used a simple neural network

with ReLU activations. Linear combinations in layers are modeled directly, while ReLUs are modeled using general max constraints, which are mixed-integer representable using linear and SOS1 [49] constraints [22].

We now show that we can model various desiderata as constraints in the MIO formulation. Given that they are constraints, we can be certain that each generated counterfactual satisfies them. The potential of MIO to formulate such constraints is well discussed in the literature [e.g., 45, 29, 36, 27], though they rarely provide a concrete formulation. We discuss MIO formulations of all considered desiderata in Appendix A.2.

Validity Let $h^{\text{raw}} : \mathcal{X} \rightarrow \mathcal{Z}$ be the neural network model $h(\cdot)$ without activation at the output layer. Let $h^{\text{raw}}(\mathbf{x}')$ be the result that we obtain from the model implementation. Assuming that we have a binary classification task ($C = 2$), a neural network typically has a single output neuron ($\mathcal{Z} = \mathbb{R}$). A sample \mathbf{x} is classified based on whether the raw output is above or below 0, i.e., $h(\mathbf{x}) = \mathbb{1}\{h^{\text{raw}}(\mathbf{x}) \geq 0\}$. Therefore, we can model the decision using the desired sign $\sigma \in \{-1, 1\}$ as

$$\sigma h^{\text{raw}}(\mathbf{x}') \geq \tau, \quad (10)$$

where $\tau \geq 0$ is a margin that can be set to ensure a higher certainty of the decision, improving the reliability of the CE. We present further specifications of validity for $C > 2$ in Appendix A.2.2.

Similarity and Sparsity To ensure similarity of the counterfactual, we follow [47, 45] and use the somewhat non-standard $\|\cdot\|_{1,\text{MAD}}$ norm, weighed by inverse Median Absolute Deviation (MAD)

$$\|\mathbf{x}\|_{1,\text{MAD}} = \sum_{j=1}^P \left| \frac{x_j}{\text{MAD}_j} \right| \quad (11)$$

$$\text{MAD}_j = \text{median}_{(\mathbf{x}, \cdot) \in \mathcal{D}} (|x_j - \text{median}_{(\mathbf{x}, \cdot) \in \mathcal{D}}(x_j)|).$$

This metric also improves sparsity and adds scale invariance that is robust to outliers [45].

Actionability and Causality Both actionability and causality depend on prior knowledge of the data. For immutability, the constraint is simply $x_j = x'_j$ for all immutable features j . We can also set the input value as a parameter instead of a variable, omitting the mixed polytope encoding. In causality, the constraints are in the form of implications [34]. We describe a way to model causal constraints where if one value changes in a certain direction, then another feature must change accordingly. This can model, among others, monotonicity, i.e., that a given value cannot decrease/increase. We call a CE *actionable* if it satisfies monotonicity and immutability constraints. Details are provided in Appendix A.2.4.

Diversity and Robustness The diversity of CEs generated by MIO is discussed in the literature [45, 36]. Although their approach can be applied to our model too, here we simply generate a set of top- M counterfactuals closest to the global optimum. We can optionally limit the maximal distance relative to the optimal CE; see the Appendix A.2.6. Regarding the robustness of the counterfactuals, Artelt et al. show that finding plausible CEs indirectly improves the robustness [2]. Thus, we do not add any further constraints to the model despite this being a viable option [e.g., 35, 27].

Plausibility Finally, we address plausibility. Artelt and Hammer are the first to use a tractable model to approximate the likelihood of a counterfactual [1]. Their formulation approximates a GMM with a quadratic term and uses a general convex optimization solver. Instead, we propose to use a trained SPN (see Section 3) that better captures categorical data, and our formulation is linear. For the SPN computation, we add the counterfactual class \hat{y}' as an additional input feature $x'_{P+1} = \hat{y}'$. Obtaining the likelihood estimate by SPN means taking the output value of the root (o_{root}). We propose two variants of utilizing this value. We can add the value to the minimization objective with some multiplicative coefficient $\alpha > 0$. We subtract this value since we wish to maximize likelihood. In experiments we use $\alpha = 0.1$ since features are normalized to $[0,1]$ and log-likelihood often takes values in the $[-100, -10]$ range.

Alternatively, we set $\alpha = 0$ and instead introduce a constraint forcing all generated CEs to have likelihood at or above a certain threshold δ^{SPN} . Such constraint is simply

$$o_{n,\text{root}} \geq \delta^{\text{SPN}}, \quad (12)$$

where δ^{SPN} is a hyperparameter of our method. Similarly to [1], we choose δ^{SPN} as the median log-likelihood of the training data, estimated by our SPN.

Full LiCE model In summary, our method optimizes the following problem:

$$\arg \min_{\mathbf{l}, \mathbf{u}, \mathbf{d}} (\mathbf{l} + \mathbf{u})^T \mathbf{v}^{\text{cont}} + (\mathbf{d} - \mathbf{d}^{\text{fact}})^T \mathbf{v}^{\text{bin}} - \alpha \cdot o_{n,\text{root}} \quad (13)$$

- s.t. mixed-polytope conditions (1–5) hold
- validity constraint (e.g., 10) holds
- SPN constraints (8–9) hold
- plausibility constraint (12) holds
- data-specific desiderata constraints hold,

where \mathbf{l} , \mathbf{u} and \mathbf{d} represent the vectors obtained by concatenation of the parameters in Eqs. 1–5. The vector \mathbf{d}^{fact} is the vector of binary variables of the encoded factual \mathbf{x} . \mathbf{v}^{cont} and \mathbf{v}^{bin} represent weights for continuous and binary variables, respectively. In our case, the weights for feature j are $1/\text{MAD}_j$ and Eq. 13 corresponds Eq. 11. Details about the data-specific constraints are in Appendix A.4.1.

Table 2: The proportion of factual instances for which a given method was able to generate a *valid* (or *actionable*) counterfactual. LiCE with a fixed likelihood bound sometimes does not generate a feasible counterfactual within the 2-minute time limit. For the other methods, it is a similar mix of inability to generate a CE or to satisfy the conditions. Overall, these results show that MIO methods have a high success rate unless the constraints are too tight. Notably, once a CE is generated, it is guaranteed to be both valid and actionable.

Method	GMSC [12]		Adult [3]		Credit [23]	
	Valid	Actionable	Valid	Actionable	Valid	Actionable
DiCE	100.0%	100.0%	99.8%	56.2%	98.4%	3.4%
VAE	1.4%	0.2%	75.4%	10.2%	27.2%	0.0%
C-CHVAE	98.6%	21.6%	16.8%	8.6%	11.0%	8.8%
FACE (ϵ)	98.6%	13.2%	62.0%	19.6%	27.2%	10.0%
FACE (knn)	98.6%	16.2%	79.4%	28.4%	27.2%	8.8%
PROPLACE	98.6%	6.6%	79.4%	6.6%	27.2%	11.8%
MIO	100.0%	100.0%	100.0%	100.0%	100.0%	100.0%
LiCE (optimize)	100.0%	100.0%	100.0%	100.0%	100.0%	100.0%
LiCE (median)	53.6%	53.6%	91.4%	91.4%	100.0%	100.0%

5 Experiments

We aim to compare the plausibility, similarity, and sparsity of counterfactuals generated by a number of methods. To quantify these criteria, we use a (negative) log-likelihood estimate using the SPN, $\|\cdot\|_{1,\text{MAD}}$, and the number of modified features, respectively.

To test the methods, we find CEs for 100 factuals. We take the factuals from both classes and look for the opposite one. For methods that can output more CEs (MIO, LiCE, DiCE, VAE), we find (at most) 10. We test for validity and actionability and measure their quality using an SPN (we use the SPFlow library [37]) trained on the same training set. Then, we select the CE with the highest estimated likelihood that is valid. If a method requires any prior training, we use the default hyperparameters (or some reasonable values for parameters without defaults, details in Appendix A.4.2) and train it on the same training set. If a given method can take into account actionability and causality constraints, we enforce them. The specific constraints for each dataset can be found in Appendix A.4.1.

We test finding counterfactuals for a simple neural network model consisting of 2 hidden layers with ReLU activations.

Data We performed tests on the Give Me Some Credit (GMSC) dataset [12], Adult dataset [3] and German Credit (referred to as Credit) dataset [23]. We dropped some outlier data and some less informative features (details in Appendix A.3) and performed all experiments in a 5-fold cross-validation setting, training each model 5 times per dataset.

Methods We compare the following CE methods:

- **MIO** represents our method without the SPN model directly formulated. We use all constraints described in Section 4, including actionability and causality constraints.
- **LiCE** is our proposed model. It is similar to MIP, with the additional plausibility constraint (Eq. 12) using the SPN. We show two variants, one with bounded log-likelihood at the median log-likelihood value on training data and another where we optimize a combination of distance and likelihood with $\alpha = 0.1$. We solve for up to 2 minutes, after which we recover (up to) 10 best solutions.
- **DiCE** is a well-known method focusing on generating a diverse set of counterfactuals [38].
- **VAE** is a method using VAE. We use the implementation available in version 0.4 of the DiCE library, based on [34].
- **C-CHVAE** uses a Conditional VAE to search for plausible (they use the term *faithful*) CEs without the need for a metric in the original space [41].
- **FACE** focuses on selecting a CE from the training set \mathcal{D} , rather than generating it from \mathcal{X} . It works by navigating a graph of the samples \mathbf{x} , where an edge exists between 2 samples if they are close (ϵ variant) or by connecting k nearest neighbors (knn variant) [44].
- **PROPLACE** is an MIO-based method for finding robust CEs within a “plausible region” constructed as a convex hull of the factual and its (robust) nearest neighbors. [27].

We use the implementations of FACE and C-CHVAE provided in the CARLA library [42]. MIO and LiCE are implemented using the open-source Pyomo modeling library [8] that allows for simple use of (almost) any MIO solver. We use the Gurobi solver [22] under an academic license. The entire implementation, together with data, is open source¹. Details about hyperparameters and other configurations of experiments are in Appendix A.4.

Results The comparison of the methods is non-trivial since factuals for which a given method generated a valid counterfactual are not the same for all methods. See Table 2 for details on the success rate of the presented methods. The lower rates are caused partly by a failure to create a counterfactual candidate at all or a failure (numerical or otherwise) to follow the validity/actionability criteria. Looking at Table 3, we notice that the proposed methods, *LiCE* and the two-stage *MIO* (generate CEs with MIO, then select using SPN), perform best not only with regards to Likelihood, but also in terms of similarity and sparsity, measured by the $\|\cdot\|_{1, \text{MAD}}$ and number of changed features, respectively. MIO-based methods are also able to generate CEs for more factuals, that is, even the more difficult ones.

DiCE, focusing on diversity, generates the least performant counterfactuals in terms of likelihood and similarity despite the use of SPN to select the most likely of the 10

¹Code is available at <https://github.com/Epanemu/LiCE>

Table 3: Mean negative log-likelihood (NLL), $\|\cdot\|_{1,\text{MAD}}$ distance, and the number of changed features, measured on *valid* generated counterfactuals for 500 testing samples from each dataset, with information about standard deviation. The log-likelihood is estimated by the SPN trained for a given fold of the 5-fold cross-validation. The number of valid counterfactuals generated by a given method varies (see Table 2), so the direct comparison between methods is non-trivial. The (+spn) means that the given method generates multiple CEs from which we choose the likeliest valid counterfactual based on the SPN. For all measures, a lower value is better.

Method	GMSC [12]			Adult [3]			Credit [23]		
	NLL ↓	Similarity ↓	Sparsity ↓	NLL ↓	Similarity ↓	Sparsity ↓	NLL ↓	Similarity ↓	Sparsity ↓
DiCE (+spn)	30.5 ± 3.7	20.7 ± 5.2	6.4 ± 1.0	20.5 ± 3.0	23.5 ± 9.9	4.6 ± 1.7	51.6 ± 17.9	28.1 ± 7.9	8.7 ± 2.2
VAE (+spn)	23.1 ± 12.6	15.4 ± 4.4	9.1 ± 0.8	17.1 ± 3.0	33.3 ± 10.9	5.5 ± 1.5	49.0 ± 17.8	28.8 ± 7.8	10.9 ± 1.8
C-CHVAE	24.9 ± 2.4	17.4 ± 4.7	9.0 ± 0.0	17.9 ± 3.2	8.6 ± 6.3	3.0 ± 1.0	34.0 ± 6.5	13.5 ± 4.9	7.6 ± 1.0
FACE (ϵ)	30.0 ± 9.0	14.8 ± 3.8	8.5 ± 1.1	16.1 ± 3.0	14.6 ± 8.4	3.7 ± 1.2	46.4 ± 17.5	18.1 ± 6.2	7.0 ± 1.2
FACE (knn)	29.5 ± 8.2	14.6 ± 3.8	8.4 ± 1.1	15.6 ± 3.1	14.1 ± 8.0	3.7 ± 1.2	44.4 ± 17.8	18.5 ± 6.2	7.1 ± 1.3
PROPLACE	27.3 ± 5.7	12.1 ± 3.1	7.4 ± 1.1	17.6 ± 3.3	22.0 ± 8.0	4.8 ± 1.2	41.2 ± 17.0	24.5 ± 6.3	8.7 ± 1.3
MIO (+spn)	27.2 ± 5.9	6.1 ± 1.8	2.7 ± 0.9	18.0 ± 3.8	5.7 ± 3.6	2.2 ± 0.9	47.5 ± 18.2	4.4 ± 2.7	2.3 ± 1.0
LiCE (opt)	25.3 ± 4.1	6.9 ± 2.5	3.0 ± 1.0	18.1 ± 3.8	5.5 ± 3.6	2.0 ± 1.0	30.3 ± 3.8	6.7 ± 3.6	2.8 ± 1.0
LiCE (med)	18.0 ± 1.8	11.3 ± 4.0	4.7 ± 1.2	12.9 ± 1.0	9.7 ± 6.5	2.9 ± 1.3	30.5 ± 3.2	6.8 ± 3.9	2.8 ± 1.1

CEs. *VAE* and *C-CHVAE* both succeed in likelihood, although this is contrasted by lower success rates, bordering with unusability. *FACE* variants have reasonable success rates for valid CEs as well as likelihood values. This is expected, since they return samples directly from the training data. Their similarity and sparsity, however, leave much to be desired. Lastly, *PROPLACE* seems to perform quite well, lagging behind LiCE and MIO in success rates (esp. lacking in actionability), but also in similarity and sparsity measures. Further comparisons and discussion of the results are in Appendices A.5 and A.6.

Limitations Our method shares the limitations of all MIO methods. The additional SPN encoding leads to some computational overhead, especially when using the likelihood threshold, as exemplified in the results on the GMSC dataset in Table 2.

6 Discussion and Conclusions

We have presented a comprehensive method for generating counterfactual explanations called LiCE. In Section 4, we show that our method satisfies the most common desiderata—namely validity, similarity, sparsity, actionability, causality, and most importantly, *plausibility*.

Our method shows promising performance at the intersection of plausibility, similarity, and sparsity. It also reliably generates high-quality, valid, and actionable CEs. However, time concerns are relevant once the full SPN is formulated within the model.

Last but not least, the Sum-Product Network encoding to MIO opens up new avenues for research.

Acknowledgement

This work has received funding from the European Union’s Horizon Europe research and innovation program under grant agreement No. 101070568.

References

- [1] André Artelt and Barbara Hammer. Convex Density Constraints for Computing Plausible Counterfactual Explanations. In Igor Farkas, Paolo Masulli, and Stefan Wermter, editors, *Artificial Neural Networks and Machine Learning – ICANN 2020*, volume 12396, pages 353–365. Springer International Publishing, Cham, 2020. ISBN 978-3-030-61608-3 978-3-030-61609-0. doi: 10.1007/978-3-030-61609-0_28.
- [2] Andre Artelt, Valerie Vaquet, Riza Velioglu, Fabian Hinder, Johannes Brinkrolf, Malte Schilling, and Barbara Hammer. Evaluating Robustness of Counterfactual Explanations. In *2021 IEEE Symposium Series on Computational Intelligence (SSCI)*, pages 01–09, Orlando, FL, USA, December 2021. IEEE. ISBN 978-1-72819-048-8. doi: 10.1109/SSCI50451.2021.9660058.
- [3] Barry Becker and Ronny Kohavi. Adult. UCI Machine Learning Repository, 1996. DOI: <https://doi.org/10.24432/C5XW20>.
- [4] Robert E Bixby. A brief history of linear and mixed-integer programming computation. *Documenta Mathematica*, 2012:107–121, 2012.
- [5] Francesco Bodria, Fosca Giannotti, Riccardo Guidotti, Francesca Naretto, Dino Pedreschi, and Salvatore Rinzivillo. Benchmarking and survey of explanation methods for black box models. *Data Mining and Knowledge Discovery*, pages 1–60, 2023.
- [6] Dieter Brughmans, Lissa Melis, and David Martens. Disagreement amongst counterfactual explanations: How transparency can be misleading. *TOP*, May 2024. ISSN 1863-8279. doi: 10.1007/s11750-024-00670-2.
- [7] Nadia Burkart and Marco F Huber. A survey on the explainability of supervised machine learning. *Journal of Artificial Intelligence Research*, 70:245–317, 2021.
- [8] Michael L Bynum, Gabriel A Hackebeil, William E Hart, Carl D Laird, Bethany L Nicholson, John D Sirola, Jean-Paul Watson, David L Woodruff, et al. *Pyomo - Optimization Modeling in Python, 3rd Edition*, volume 67. Springer, 2021.
- [9] Ruth M. J. Byrne. *The Rational Imagination: How People Create Alternatives to Reality*. The MIT Press, June 2005. ISBN 978-0-262-26962-9. doi: 10.7551/mitpress/5756.001.0001.
- [10] F. Ceccon, J. Jalving, J. Haddad, A. Thebelt, C. Tsay, C. D Laird, and R. Misener. OMLT: Optimization & machine learning toolkit. *Journal of Machine Learning Research*, 23(349):1–8, 2022.

- [11] YooJung Choi, Antonio Vergari, and Guy Van den Broeck. Probabilistic circuits: A unifying framework for tractable probabilistic models. *UCLA*, October 2020.
- [12] Will Cukierski Credit Fusion. Give me some credit, 2011.
- [13] Zhicheng Cui, Wenlin Chen, Yujie He, and Yixin Chen. Optimal Action Extraction for Random Forests and Boosted Trees. In *Proceedings of the 21th ACM SIGKDD International Conference on Knowledge Discovery and Data Mining*, pages 179–188, Sydney NSW Australia, August 2015. ACM. ISBN 978-1-4503-3664-2. doi: 10.1145/2783258.2783281.
- [14] Rudresh Dwivedi, Devam Dave, Het Naik, Smiti Singhal, Rana Omer, Pankesh Patel, Bin Qian, Zhenyu Wen, Tejal Shah, Graham Morgan, and Rajiv Ranjan. Explainable AI (XAI): Core Ideas, Techniques, and Solutions. *ACM Computing Surveys*, 55(9):194:1–194:33, January 2023. ISSN 0360-0300. doi: 10.1145/3561048.
- [15] Equal Credit Opportunity Act (ECOA). Equal Credit Opportunity Act (ECOA). <https://www.law.cornell.edu/uscode/text/15/chapter-41/subchapter-IV>, 1974. Title 15 of the United States Code, Chapter 41, Subchapter IV, paragraph 1691 and following.
- [16] European Commission. Directive 2013/36/EU of the European Parliament and of the Council of 26 June 2013 on access to the activity of credit institutions and the prudential supervision of credit institutions and investment firms, amending Directive 2002/87/EC and repealing Directives 2006/48/EC and 2006/49/EC., 2016. URL <https://eur-lex.europa.eu/legal-content/EN/TXT/?uri=celex%3A32013L0036>. Accessed: 2023-04-30.
- [17] European Commission. Regulation (EU) 2016/679 of the European Parliament and of the Council of 27 April 2016 on the protection of natural persons with regard to the processing of personal data and on the free movement of such data, and repealing Directive 95/46/EC (General Data Protection Regulation), 2016. URL <https://eur-lex.europa.eu/eli/reg/2016/679/oj>. Accessed: 2023-04-30.
- [18] Robert Gens and Pedro Domingos. Learning the structure of sum-product networks. In *Proceedings of the 30th International Conference on International Conference on Machine Learning - Volume 28*, ICML'13, page III–873–III–880. JMLR.org, 2013.
- [19] Noam Goldberg, Steffen Rebennack, Youngdae Kim, Vitaliy Krasko, and Sven Leyffer. MINLP formulations for continuous piecewise linear function fitting. *Computational Optimization and Applications*, 79(1):223–233, May 2021. ISSN 1573-2894. doi: 10.1007/s10589-021-00268-5.
- [20] Riccardo Guidotti. Counterfactual explanations and how to find them: Literature review and benchmarking. *Data Mining and Knowledge Discovery*, April 2022. ISSN 1573-756X. doi: 10.1007/s10618-022-00831-6.

- [21] David Gunning. Broad agency announcement explainable artificial intelligence (xai). Technical report, DARPA, August 2016.
- [22] Gurobi Optimization, LLC. Gurobi optimizer reference manual, 2023.
- [23] Hans Hofmann. Statlog (German Credit Data), 1994.
- [24] Joey Huchette and Juan Pablo Vielma. Nonconvex Piecewise Linear Functions: Advanced Formulations and Simple Modeling Tools. *Operations Research*, 71(5):1835–1856, September 2023. ISSN 0030-364X. doi: 10.1287/opre.2019.1973.
- [25] Joey Huchette, Gonzalo Muñoz, Thiago Serra, and Calvin Tsay. When deep learning meets polyhedral theory: A survey. *arXiv preprint arXiv:2305.00241*, 2023.
- [26] Junqi Jiang, Francesco Leofante, Antonio Rago, and Francesca Toni. Formalising the robustness of counterfactual explanations for neural networks. *Proceedings of the AAAI Conference on Artificial Intelligence*, 37(12):14901–14909, June 2023. doi: 10.1609/aaai.v37i12.26740.
- [27] Junqi Jiang, Jianglin Lan, Francesco Leofante, Antonio Rago, and Francesca Toni. Provably Robust and Plausible Counterfactual Explanations for Neural Networks via Robust Optimisation. In *Proceedings of the 15th Asian Conference on Machine Learning*, pages 582–597. PMLR, February 2024.
- [28] Michael I Jordan, Zoubin Ghahramani, Tommi S Jaakkola, and Lawrence K Saul. An introduction to variational methods for graphical models. *Learning in graphical models*, pages 105–161, 1998.
- [29] Kentaro Kanamori, Takuya Takagi, Ken Kobayashi, and Hiroki Arimura. DACE: Distribution-Aware Counterfactual Explanation by Mixed-Integer Linear Optimization. In *Proceedings of the Twenty-Ninth International Joint Conference on Artificial Intelligence*, pages 2855–2862, Yokohama, Japan, July 2020. International Joint Conferences on Artificial Intelligence Organization. ISBN 978-0-9992411-6-5. doi: 10.24963/ijcai.2020/395.
- [30] Amir-Hossein Karimi, Gilles Barthe, Bernhard Schölkopf, and Isabel Valera. A survey of algorithmic recourse: definitions, formulations, solutions, and prospects. *arXiv preprint arXiv:2010.04050*, 2020.
- [31] Amir-Hossein Karimi, Bernhard Schölkopf, and Isabel Valera. Algorithmic recourse: from counterfactual explanations to interventions. In *Proceedings of the 2021 ACM conference on fairness, accountability, and transparency*, pages 353–362, 2021.
- [32] Diederik P. Kingma and Max Welling. Auto-Encoding Variational Bayes, December 2022.

- [33] Bo Li, Peng Qi, Bo Liu, Shuai Di, Jingen Liu, Jiquan Pei, Jinfeng Yi, and Bowen Zhou. Trustworthy AI: From Principles to Practices. *ACM Computing Surveys*, 55(9):177:1–177:46, January 2023. ISSN 0360-0300. doi: 10.1145/3555803.
- [34] Divyat Mahajan, Chenhao Tan, and Amit Sharma. Preserving Causal Constraints in Counterfactual Explanations for Machine Learning Classifiers, June 2020.
- [35] Donato Maragno, Jannis Kurtz, Tabea E. Röber, Rob Goedhart, Ş Ilker Birbil, and Dick den Hertog. Finding Regions of Counterfactual Explanations via Robust Optimization, May 2023.
- [36] Kiarash Mohammadi, Amir-Hossein Karimi, Gilles Barthe, and Isabel Valera. Scaling Guarantees for Nearest Counterfactual Explanations. In *Proceedings of the 2021 AAAI/ACM Conference on AI, Ethics, and Society*, AIES ’21, pages 177–187, New York, NY, USA, July 2021. Association for Computing Machinery. ISBN 978-1-4503-8473-5. doi: 10.1145/3461702.3462514.
- [37] Alejandro Molina, Antonio Vergari, Karl Stelzner, Robert Peharz, Pranav Subramani, Nicola Di Mauro, Pascal Poupart, and Kristian Kersting. Spflow: An easy and extensible library for deep probabilistic learning using sum-product networks, 2019.
- [38] Ramaravind Kommiya Mothilal, Amit Sharma, and Chenhao Tan. Explaining Machine Learning Classifiers through Diverse Counterfactual Explanations. In *Proceedings of the 2020 Conference on Fairness, Accountability, and Transparency*, pages 607–617, January 2020. doi: 10.1145/3351095.3372850.
- [39] Christos H Papadimitriou. On the complexity of integer programming. *Journal of the ACM (JACM)*, 28(4):765–768, 1981.
- [40] Axel Parmentier and Thibaut Vidal. Optimal Counterfactual Explanations in Tree Ensembles. In *Proceedings of the 38th International Conference on Machine Learning*, pages 8422–8431. PMLR, July 2021.
- [41] Martin Pawelczyk, Klaus Broelemann, and Gjergji Kasneci. Learning Model-Agnostic Counterfactual Explanations for Tabular Data. In *Proceedings of The Web Conference 2020*, WWW ’20, pages 3126–3132, New York, NY, USA, April 2020. Association for Computing Machinery. ISBN 978-1-4503-7023-3. doi: 10.1145/3366423.3380087.
- [42] Martin Pawelczyk, Sascha Bielawski, Johannes van den Heuvel, Tobias Richter, and Gjergji Kasneci. CARLA: A python library to benchmark algorithmic recourse and counterfactual explanation algorithms, 2021.
- [43] Hoifung Poon and Pedro Domingos. Sum-product networks: A new deep architecture. In *2011 IEEE International Conference on Computer Vision Workshops (ICCV Workshops)*, pages 689–690, November 2011. doi: 10.1109/ICCVW.2011.6130310.

- [44] Rafael Poyiadzi, Kacper Sokol, Raul Santos-Rodriguez, Tijl De Bie, and Peter Flach. FACE: Feasible and Actionable Counterfactual Explanations. In *Proceedings of the AAAI/ACM Conference on AI, Ethics, and Society*, pages 344–350, February 2020. doi: 10.1145/3375627.3375850.
- [45] Chris Russell. Efficient Search for Diverse Coherent Explanations. In *Proceedings of the Conference on Fairness, Accountability, and Transparency, FAT* '19*, pages 20–28, New York, NY, USA, January 2019. Association for Computing Machinery. ISBN 978-1-4503-6125-5. doi: 10.1145/3287560.3287569.
- [46] Berk Ustun, Alexander Spangher, and Yang Liu. Actionable Recourse in Linear Classification. In *Proceedings of the Conference on Fairness, Accountability, and Transparency*, pages 10–19, Atlanta GA USA, January 2019. ACM. ISBN 978-1-4503-6125-5. doi: 10.1145/3287560.3287566.
- [47] Sandra Wachter, Brent Mittelstadt, and Chris Russell. Counterfactual Explanations Without Opening the Black Box: Automated Decisions and the GDPR. *SSRN Electronic Journal*, 2017. ISSN 1556-5068. doi: 10.2139/ssrn.3063289.
- [48] H Paul Williams. *Model building in mathematical programming*. John Wiley & Sons, 2013.
- [49] Laurence A Wolsey. *Integer programming*. John Wiley & Sons, 2020.
- [50] Riting Xia, Yan Zhang, Xueyan Liu, and Bo Yang. A survey of sum-product networks structural learning. *Neural Networks*, 2023.
- [51] Songming Zhang, Xiaofeng Chen, Shiping Wen, and Zhongshan Li. Density-based reliable and robust explainer for counterfactual explanation. *Expert Systems with Applications*, 226:120214, September 2023. ISSN 0957-4174. doi: 10.1016/j.eswa.2023.120214.

A Appendix

A.1 Notation

Generally, notation follows these rules:

- Capital letters typically refer to amounts of something, as in classes, features, bins, etc. Exceptions are U , L , and F , which are taken from the original work [45].
- Caligraphic capital letters denote sets or continuous spaces.
- Small Latin letters are used as indices, variables, or parameters of the MIP formulation.
- Small Greek letters refer to hyperparameters of the LiCE formulation or parameters of the SPN (scope ψ , parameters θ).
- Subscript is used to specify the position of a scalar value in a matrix or a vector. When in parentheses, it specifies the index of a vector within a set.
- Superscript letters refer to a specification of a symbol with otherwise intuitively similar meaning. Except for \mathbb{R}^P , where P has the standard meaning of P -dimensional.
- A hat ($\hat{\cdot}$) symbol above a variable means that the variable is the output of the Neural Network $h(\cdot)$.
- A prime ($'$) symbol as a superscript of a variable means that the variable is a part of (or the output of) the counterfactual.
- In bold font are only vectors. When we work with a scalar value, the symbol is in regular font.

The specific meanings of symbols used in the article are shown in Tables 4 to 8. The symbols are divided into groups.

- Functions non-specific to our task (Table 4)
- Used indices (Table 5)
- LiCE (hyper)parameters that can be tuned (Table 6)
- Classification task and SPN symbols (Table 7)
- MIO formulation parameters and variables (Table 8)

Table 4: General functions used

General function symbols	
$ \cdot $	Absolute value (if scalar) or size of the set
$[\cdot]$	Set of integers, $[N] = \{1, 2, \dots, N\}$
$\mathbb{1}\{\cdot\}$	Equal 1 if input is true, 0 otherwise
$\ \cdot\ _0$	ℓ_0 norm, number of non-zero elements
$2^{[P]}$	Set of all subsets of $[P]$

Table 5: Symbols used as indices

Indices	
j	Index of features, typically $j \in [P]$
(m)	Index of counterfactuals within a set \mathcal{C}_x , typically $m \in [M]$
n	A node of the SPN, $n \in \mathcal{V}$
i	Index of bins of a histogram in a leaf node (n), typically $i \in [B_n]$
a	A predecessor node (of node n) in the SPN, usually $a \in \text{pred}(n)$
k	A class ($k \in [C]$) or categorical value ($k \in [K_j]$) index
e	Index of the feature that is changed as an effect of causal relation R

A.2 MIO formulations

The following MIO formulations of the desiderata are novel in that we came up with them, and, to the best of our knowledge, they were not formalized before. They are not too complex, but we formulate them for completeness.

A reasonable value of α is 0.1 since features are normalized to $[0,1]$ and log-likelihood often takes values in the $[-100, -10]$ range.

A.2.1 SPN histogram formulation

In practice, the probability distribution of a leaf $n \in \mathcal{V}^L$ trained on data is a histogram on a single feature j , i.e., $\psi(n) = \{j\}$. The interval of possible values of x'_j is split into B_n bins, delimited by $B_n + 1$ breakpoints denoted $t_{n,i}$, $i \in [B_n + 1]$.

Because modeling that a variable belongs to a union of intervals is simpler than an intersection, we consider variables $\bar{b}_{n,i}$ that equal 1 if and only if the value x'_j does *not*

Table 6: Input parameters into the LiCE formulation

LiCE (hyper)parameters	
σ	Desired sign of counterfactual for binary classification. $\sigma = -1$ corresponds to class 0 and $\sigma = 1$ to class 1.
τ	The minimal difference between counterfactual class ($h^{\text{raw}}(\mathbf{x}')_{\hat{y}'}$) and factual class ($h^{\text{raw}}(\mathbf{x}')_{\hat{y}}$) NN output value. Alternatively, for binary classification, it is the requirement for a minimal absolute value of the NN output before sigmoid activation ($h^{\text{raw}}(\mathbf{x}')$).
ρ	Limit for the relative difference of values of the objective function within the set of closest counterfactuals $\mathcal{C}_{\mathbf{x}}$.
α	Weight of negative log-likelihood in the objective function
ϵ_j	Minimal change in continuous value c_j of j -th feature. The absolute difference between x'_j and x_j is either 0, or at least ϵ_j .
δ^{SPN}	Lower bound on the estimated value of likelihood of the generated counterfactual.

belong to the interval $[t_{n,i}, t_{n,i+1})$. This leads to a set of constraints

$$\bar{b}_{n,i} \geq t_{n,i} - x'_j \quad \forall n \in \mathcal{V}^L, \forall i \in [B_n] \quad (14)$$

$$\bar{b}_{n,i} \geq x'_j + \epsilon_j - t_{n,i+1} \quad \forall n \in \mathcal{V}^L, \forall i \in [B_n] \quad (15)$$

$$\sum_{i=1}^{B_n} \bar{b}_{n,i} = B_n - 1 \quad \forall n \in \mathcal{V}^L \quad (16)$$

$$o_n = \sum_{i=1}^{B_n} (1 - \bar{b}_{n,i}) \log q_{n,i} \quad \forall n \in \mathcal{V}^L \quad (17)$$

$$\bar{b}_{n,i} \in \{0, 1\} \quad \forall n \in \mathcal{V}^L, \forall i \in [B_n], \quad (18)$$

where $q_{n,i}$ is the likelihood value in a bin i and o_n is the output value of the leaf node n . ϵ_j is again the minimal change in the feature j and ensures that we consider an open interval on one side. We use the fact that all values x_j (thus also $t_{n,i}$) are in the interval $[0, 1]$. Eq. 14 sets $\bar{b}_{n,i} = 1$ if $x'_j < t_{n,i}$ and Eq. 15 sets $\bar{b}_{n,i} = 1$ for values on the other side of the bin $x'_j \geq t_{n,i+1}$. Eq. 16 ensures that a single bin is chosen and Eq. 17 sets the output value to the log value of the bin that \mathbf{x}' belongs to. This implementation of bin splitting is inspired by the formulation of interval splitting in piecewise function fitting [19].

We assume that the bins cover the entire space, which we can ensure by adding at most 2 bins on both sides of the interval.

A.2.2 Validity

For $C > 2$ classes, the raw output has C dimensions ($\mathcal{Z} = \mathbb{R}^C$), and the classifier assigns the class equal to the index of the highest value, i.e., $h(\mathbf{x}) = \arg \max_{k \in [C]} h^{\text{raw}}(\mathbf{x})_k$.

Table 7: Symbols of the classification task, CE search, and SPNs

Classification task symbols	
P	Number of features
C	Number of classes
\mathcal{D}	The dataset, set of 2-tuples $(\mathbf{x}, y) \in \mathcal{D}$
\mathcal{X}	Input space $\mathcal{X} \subseteq \mathbb{R}^P$
\mathbf{x}	A (factual) sample $\mathbf{x} \in \mathcal{X}$
x_j	A j -th feature of sample \mathbf{x}
y	Ground truth of sample \mathbf{x} , $y \in [C]$
$h(\cdot)$	Classifier we are explaining $h : \mathcal{X} \rightarrow [C]$
\hat{y}	Classifier-predicted class $h(\mathbf{x}) = \hat{y} \in [C]$
$h^{\text{raw}}(\cdot)$	NN classifier output without activation $h^{\text{raw}} : \mathcal{X} \rightarrow \mathcal{Z}$
\mathcal{Z}	Output space of the NN classifier, without sigmoid/softmax activation
Counterfactual generation symbols	
$\ \cdot\ _{1,\text{MAD}}$	Counterfactual distance function (see Eq. 11)
$\mathcal{C}_{\mathbf{x}}$	Set of generated counterfactuals for factual \mathbf{x}
M	Number of sought counterfactuals, $M \geq \mathcal{C}_{\mathbf{x}} $
\mathbf{x}'	Counterfactual explanation of \mathbf{x} , $\mathbf{x}' \in \mathcal{C}_{\mathbf{x}}$
\mathbf{x}'^*	Optimal (closest) counterfactual
$\mathbf{x}'_{(m)}$	m -th counterfactual explanation of factual \mathbf{x}
x'_j	A value of j -th feature of the counterfactual
\hat{y}'	Predicted class of the counterfactual (can be a parameter of LiCE)
Sum Product Network symbols	
\mathcal{V}	Set of nodes of the SPN
\mathcal{V}^L	Set of leaf nodes
\mathcal{V}^Σ	Set of sum nodes
\mathcal{V}^Π	Set of product nodes
$\text{pred}(\cdot)$	Function returning children (predecessors) of a node
$\psi(\cdot)$	Scope function mapping nodes to their input features $\psi : \mathcal{V} \rightarrow 2^{[P]}$
θ	Parameters of the SPN
O_n	Output value of a node $n \in \mathcal{V}$
$w_{a,n}$	Weight of output value of predecessor node a in computing the value of sum node n .
n^{root}	Root node, its value is the value of the SPN

Table 8: Used variables and parameters in the MIO formulation

MIO formulation variables	
l_j	Decrease in continuous value of j -th feature.
\mathbf{l}	Concatenated vector of all l_j .
u_j	Increase in continuous value of j -th feature.
\mathbf{u}	Concatenated vector of all u_j .
c_j	Continuous value of j -th CE feature.
$d_{j,k}$	1 iff x'_j takes k -th categorical value $k \in K_j$.
\mathbf{d}	All variables $d_{j,k}$ concatenated into a vector.
d_j^{cont}	1 iff x'_j takes continuous value c_j .
$h^{\text{raw}}(\cdot)_k$	Value of h^{raw} , corresponding to class $k \in [C]$.
g_k	1 iff class $k \in [C]$ has higher h^{raw} value than the factual class.
s_j	1 iff j -th feature changed, i.e., $x_j \neq x'_j$.
r	1 iff causal relation R is activated, i.e., cause is satisfied and effect is enforced.
$\bar{b}_{n,i}$	1 iff x'_j does <i>not</i> belong to the i -th bin ($i \in [B_n]$), assuming j -th feature corresponds to node n , i.e., $\psi(n) = \{j\}$.
o_n	Estimated output value of SPN node $n \in \mathcal{V}$.
MIO formulation parameters	
L_j	Lower bound on continuous values of j -th feature. In our implementation, equal to 0.
U_j	Upper bound on continuous values of j -th feature. In our implementation, equal to 1.
F_j	Default continuous value of j -th feature, equal to the value of the factual x_j , if it has continuous value. Otherwise equal to the median.
K_j	Number of categorical values of j -th feature.
f_j	Equal to x_j , if it has categorical value. If x_j is continuous, f_j is removed, and so are all constraints containing it.
S	Maximal number of feature value changes of \mathbf{x}' compared to \mathbf{x} . Sparsity limit.
R	Example causal relation: if j -th feature increases, e -th feature must decrease.
B_n	Number of bins in the histogram of leaf node n .
$t_{n,i}$	Threshold between $i - 1$ -th and i -th bin in histogram of leaf node n .
$q_{n,i}$	Likelihood value of i -th bin of node n .
\mathbf{v}^{bin}	Vector of respective $\ \cdot\ _{1,\text{MAD}}$ weights for binary one-hot encodings.
\mathbf{v}^{cont}	Vector of respective $\ \cdot\ _{1,\text{MAD}}$ weights for continuous values.
\mathbf{d}^{fact}	One-hot encoded vector of factual categorical values corresponding to \mathbf{d} .

Let \hat{y}' be the desired counterfactual class. The validity constraint, given that we specify the counterfactual class prior, is then

$$h^{\text{raw}}(\mathbf{x}')_{\hat{y}'} - h^{\text{raw}}(\mathbf{x}')_k \geq \tau \quad \forall k \in [C] \setminus \{\hat{y}'\}. \quad (19)$$

Note that we can also implement a version where we do not care about the counterfactual class \hat{y}' in advance by the following

$$\begin{aligned} g_k = 1 &\implies h^{\text{raw}}(\mathbf{x}')_k - h^{\text{raw}}(\mathbf{x}')_{\hat{y}} \geq \tau \quad \forall k \in [C] \setminus \{\hat{y}\} \\ g_k = 0 &\implies h^{\text{raw}}(\mathbf{x}')_k - h^{\text{raw}}(\mathbf{x}')_{\hat{y}} \leq \tau \quad \forall k \in [C] \setminus \{\hat{y}\} \\ &\sum_{k \in [C] \setminus \{\hat{y}\}} g_k \geq 1, \end{aligned} \quad (20)$$

where \implies can be seen either as an indicator constraint or as an implication [48], g_k is equal to 1 if and only if class k has a higher value than the factual class \hat{y} in the raw output. The sum then ensures that at least one other class has a higher value.

A wide variety of constraints ensuring validity are possible. For example, we can ensure that the factual class has the lowest score by setting $\sum_{k \in [C] \setminus \{\hat{y}\}} g_k \geq C - 1$, or we could enforce a custom order of classes.

A.2.3 Sparsity

To constrain the sparsity further, we can set an upper bound S on the number of features changed

$$\begin{aligned} \sum_j s_j &\leq S \\ s_j &\geq 1 - d_{j,f_j} && \forall j \in [P] \\ s_j &\geq d_{j,k} && \forall j \in [P], \forall k \in [K_j] \setminus \{f_j\} \\ s_j &\geq l_j + u_j && \forall j \in [P] \\ s_j &\in \{0, 1\} && \forall j \in [P], \end{aligned} \quad (21)$$

where we use the binary value s_j that equals 1 if the j -th feature changed, the f_j is the categorical value of attribute j of the factual (if applicable).

Neither LiCE nor MIO use this constraint.

A.2.4 Causality

Consider the following example of a causal relation R . If feature j increases its value, another feature e must decrease. For continuous ranges, this is formulated as

$$\begin{aligned} r &\geq u_j - l_j \\ l_e &\geq r \epsilon_e \\ u_e &\leq 1 - r \\ r &\in \{0, 1\}, \end{aligned} \quad (22)$$

where ϵ_e is a minimal change in the value of feature e and r equals 1 if the relation R is active. In the case when the features are ordinal, we can assume that their values are just categorical one-hot encoded variables ordered by indices and use:

$$\begin{aligned}
r &\geq \sum_{k=f_j+1}^{K_j} d_{j,k} \\
r &\leq \sum_{k=1}^{f_e} d_{e,k} \\
r &\in \{0, 1\},
\end{aligned} \tag{23}$$

where f_j is the categorical value of the factual in feature j . Naturally, one can see that we can use any combination of increasing/decreasing values in continuous and categorical feature spaces. With these formulations, we can also model monotone values, such as age or education. We simply replace the variable r by 1.

A.2.5 Complex data

We use the umbrella term ‘‘Complex data’’ to refer to tabular data with non-real continuous values. This includes categorical (e.g., race), binary (e.g., migrant status), ordinal (e.g., education), and discrete contiguous (e.g., number of children) values.

For binary, we use a simple 0-1 encoding; categorical data is encoded into one-hot vectors; and discrete variables are discretized by fixing their value to an integer variable within the formulation. Since we normalize all values to the $[0, 1]$ range, we use a proxy integer variable m :

$$\begin{aligned}
(F_j - l_j + u_j) * \text{scale}_j + \text{shift}_j &= m \\
m &\in \mathbb{Z}
\end{aligned}$$

For ordinal variables, we use the same encoding as categorical values, with the addition of the one-hot encoding being sorted by value rank to allow for the causality/monotonicity to be enforced.

A.2.6 Diversity

Instead of a single counterfactual, the solver returns (up to) M counterfactuals closest to the global optimum, optionally within some distance range. This range is defined in terms of the objective function, which is the distance of a counterfactual in our case. In other words, we search for a set $\mathcal{C}_{\mathbf{x}} = \{\mathbf{x}'_{(1)}, \dots, \mathbf{x}'_{(M)}\}$ of counterfactuals that have a similar distance to the factual.

Let \mathbf{x}'^* be the closest CE satisfying all other constraints; we can set a parameter ρ that represents the relative distance of all CEs to the \mathbf{x}'^* leading to the generation of set

$$\mathcal{C}_{\mathbf{x}} = \{\mathbf{x}' \mid \|\mathbf{x} - \mathbf{x}'\|_{1,\text{MAD}} \leq (1 + \rho) \cdot \|\mathbf{x} - \mathbf{x}'^*\|_{1,\text{MAD}}\}.$$

Nevertheless, we disregard the relative distance parameter and search for the M closest CEs. Later, we sift through the set \mathcal{C} of top- M counterfactuals, looking for the most likely CEs. Here, one could perform any filtering.

A.3 Data modifications

We always remove samples with missing values. Optionally, we also remove some outlier data or uninformative features.

GMSC We do not remove any feature in GMSC, but we keep only data with reasonable values to avoid numerical issues within MIO. The thresholds for keeping the sample are as follows

- `MonthlyIncome < 50000`
- `RevolvingUtilizationOfUnsecuredLines < 1`
- `NumberOfTime30-59DaysPastDueNotWorse < 10`
- `DebtRatio < 2`
- `NumberOfOpenCreditLinesAndLoans < 40`
- `NumberOfTimes90DaysLate < 10`
- `NumberRealEstateLoansOrLines < 10`
- `NumberOfTime60-89DaysPastDueNotWorse < 10`
- `NumberOfDependents < 10`

this removes around 5.5% of data after data with missing values was removed. We could combat the same issues by taking a log of some of the features. In our “pruned” GMSC dataset, there are 113,595 samples and 10 features, none of which are categorical, 7 are discrete contiguous, and the remaining 3 are real continuous. Further details are in the preprocessing code.

Adult In the Adult dataset, we remove 5 features

- `fnlwgt` which equals the estimated number of people the data sample represents in the census, and is thus not actionable and difficult to obtain for new data, making it less useful for predictions,
- `education-num` because it can be substituted by ordinal feature `education`,
- `native-country` because it is again not actionable, less informative, and also heavily imbalanced,
- `capital-gain` and `capital-loss` because they contain few non-zero values.

It is not uncommon to remove the features we did, as some of them also have many missing values. We remove only about 2% of the data by removing samples with missing values. We are left with 47,876 samples and 9 features, 5 of which are categorical, 1 is binary, 1 ordinal, and the remaining 2 are discrete contiguous. Further details are in the preprocessing code.

Credit We do not remove any samples or features for the Credit dataset. The dataset contains 1,000 samples and 20 features, 10 of which are categorical, 2 are binary, 1 ordinal, 5 are discrete contiguous, and the remaining 2 are real continuous. Further details are in the preprocessing code.

All code used for the data preprocessing is in the supplementary material.

A.4 Experiment setup

Here, we describe the details of our experiments. The code used for experiments with examples is in the supplementary material and will be made available once the paper is accepted.

A.4.1 Additional Constraints

In addition to data type constraints described in Section A.3, we also constrain some features for immutability and causality.

GMSC

- **Immutable:** `NumberOfDependents`
- **Monotone:** `age` cannot decrease
- **Causal:** no constraints

Adult

- **Immutable:** `race` and `sex`
- **Monotone:** `age` cannot decrease and `education` cannot decrease
- **Causal:** `education increases` \implies `age increases`

Credit

- **Immutable:** `Number of people being liable to provide maintenance for`, `Personal status` and `sex`, and `foreign worker`
- **Monotone:** `Age` cannot decrease
- **Causal:** `Present residence since increases` \implies `Age increases` and `Present employment since increases` \implies `Age increases`

A.4.2 Hyperparameter setup

The entire configuration can be found in the code, but we also present (most of) it here.

Neural Network We compare methods on a neural network with four layers, first with a size equal to the length of the encoded input, then 20 and 10 for hidden layers, and a single neuron as output. It trained with batch size 64 for 50 epochs. We compare all methods on this neural network architecture, trained separately five times for each training set (from the five folds).

SPN To create fewer nodes in the SPN (i.e., to not overtrain it), we set the `min_instances_slice` parameter to the number of samples divided by 20.

CE methods We used default parameters for most methods. In cases when there were no default values set, we used the following:

- *DiCE*: we use the gradient method of searching for CEs.
- *VAE*: we set the size of the model to copy the predictor model. We parametrize the hinge loss with a margin of 0.1 and multiply the validity loss by 10 to promote validity. We use learning rate 1e-3 and batch size 64. We use weight decay of 1e-4 and train for 20 epochs (200 for the Credit data since the dataset is small).
- *FACE*: we only configure the fraction of the dataset used to search for the CE, increasing it to 0.5 for the Credit dataset due to its size.
- *C-CHVAE*: we set the size of the model to copy the predictor model. For the Credit dataset, we increase the number of training epochs to 50.
- *PROPLACE*: We create the retrained NN models to reflect the same architecture and train them for 15 epochs. We set up 1 instance of PROPLACE per class and set its delta by starting at 0.025 and decreasing by 0.005 until we are able to recover enough samples.
- *LiCE + MIO*: For our methods, we configure a time limit of 2 minutes for MIO solving. These are well enough for MIO, but LiCE tends to struggle with increasing likelihood requirements. We generate 10 closest CEs, not using the relative distance parameter. We set the decision margin $\tau = 10^{-4}$ and we use one $\epsilon_j = 10^{-4}$ for all features j because they are normalized. We choose δ^{SPN} equal to the median (or lower quartile) of likelihood on the dataset.

A.4.3 Computational resources

Most experiments ran on a personal laptop with 32GB of RAM and 16 CPUs AMD Ryzen 7 PRO 6850U, but since the proposed methods had undergone wider experimentation, their experiments were run on an internal cluster with assigned 32GB of RAM and 16 CPUs, some AMD EPYC 7543 and some Intel Xeon Scalable Gold 6146, based on their availability.

Regarding computational time, it is non-trivial to estimate. The time varies greatly for some methods since, for example, VAE retries generating a CE until a valid is found or a limit on tries is reached. Most methods we compared took a few hours for the 500 samples, including the method training. The MIO method takes, on average, a few

Table 9: Comparison of LiCE variants. (optimize) means that we optimize the likelihood together with the distance, with coefficient $\alpha = 0.1$. (quartile) means that we constrain the CE to have the likelihood greater or equal to the lower quartile likelihood of training data. Finally, (median) is the same as (quartile), but we take the median instead of the quartile.

Method	GMSC			Adult			Credit		
	NLL	Similarity	Sparsity	NLL	Similarity	Sparsity	NLL	Similarity	Sparsity
MIO (+spn)	27.2 ± 5.9	6.1 ± 1.8	2.7 ± 0.9	18.0 ± 3.8	5.7 ± 3.6	2.2 ± 0.9	47.5 ± 18.2	4.4 ± 2.7	2.3 ± 1.0
LiCE (optimize)	25.3 ± 4.1	6.9 ± 2.5	3.0 ± 1.0	18.1 ± 3.8	5.5 ± 3.6	2.0 ± 1.0	30.3 ± 3.8	6.7 ± 3.6	2.8 ± 1.0
LiCE (quartile)	26.3 ± 2.9	6.9 ± 2.5	2.5 ± 0.9	18.4 ± 3.5	5.6 ± 3.8	2.0 ± 1.0	31.1 ± 4.2	6.6 ± 3.6	2.6 ± 1.0
LiCE (median)	18.0 ± 1.8	11.3 ± 4.0	4.7 ± 1.2	12.9 ± 1.0	9.7 ± 6.5	2.9 ± 1.3	30.5 ± 3.2	6.8 ± 3.9	2.8 ± 1.1

seconds to generate an optimal counterfactual, while LiCE often reaches the 2-minute time limit.

Considering the tests presented in this paper, we estimate 200 hours of real-time was spent generating them, meaning approximately 3,200 CPU hours. If we include all preliminary testing, the compute time is estimated at around 15,000 CPU hours, though these are all inaccurate rough estimates, given that the hours were not tracked.

A.5 Further comparisons

In this section, we would like to discuss some results that could not fit into the article’s main body.

A.5.1 LiCE variants

We tested multiple versions of using the SPN within LiCE. In Table 9, we show results

The results show that selecting the most likely CE out of 10 local optima given by MIO is surprisingly strong. [SHOW WITHOUT THE SELECTION] A two-stage setup can be quite performant. The results on similarity show that some of the MIO CEs are not globally optimal. This happens likely because the SPN in the second phase selects some of the locally optimal CEs.

A.5.2 Time concerns

Table 10 shows the median number of seconds required to generate (or fail to generate) a CE. We see that there are stark differences between methods and also between datasets. For methods using MIO, we constrain the maximal solution time to 120 seconds.

LiCE seems to be comparable on Adult as well as Credit datasets. Seeing that MIO seems to have better time complexity, we suggest that the main portion of the overhead is caused by solving the SPN formulation. Please note that the optimizing variant of LiCE takes long mainly to prove optimality. A (non-optimal) solution could likely be obtained even with a tighter time limit. [SAVE LOGS OF THE OPTIMIZATION and find out the numbers for this]

Table 10: Median time spent on the computation of a single CE. The values significantly above 120 in the LiCE computation on GMSC are partly caused by computational overhead in formulating the SPN and partly possibly by a mistake in the computation of the values. Time spent optimizing was limited to 120 seconds, as reflected in the LiCE duration on the Credit dataset.

Method	GMSC	Adult	Credit
DiCE (+spn)	25.27s	17.04s	147.35s
VAE (+spn)	0.64s	0.97s	0.63s
C-CHVAE	0.43s	0.63s	0.59s
FACE (ϵ)	7.88s	7.46s	5.12s
FACE (knn)	5.65s	7.41s	5.28s
PROPLACE	0.38s	0.24s	0.20s
MIO	0.25s	0.36s	0.41s
LiCE (optimize)	122.89s	28.16s	0.87s
LiCE (median)	122.27s	8.08s	0.81s

A.5.3 Other plausibility metrics

We considered using Kernel Density Estimator (KDE) for the evaluation (similarly to [1]), but the KDE does not perform well on categorical data, so we decided against it.

A.6 Further comments

Given the limited size of the Credit dataset, it is unsurprising to see so many failures of some methods. There is not much data for some methods to support the training. This might be behind the low success rate of computing a valid CE.

Regarding the other results, it is possible that the VAE method has been misconfigured for GMSC, returning very few results.

It is unclear why there is a drop in the success rate for Valid and Actionable results for the MIO-based methods. It could be caused by numerical inaccuracies, but mainly, it is important to note that despite a drop in success rate, the difference compared to other methods is significant.

The main disadvantage of LiCE is the time complexity of CE generation. This will be studied further, hopefully leading to improvement. We argue, however, that for some use cases, the user might be willing to wait to obtain a high-quality CE. We leave this decision of usefulness to the user.

A.6.1 Omitted methods

It is not in our power to test against all CE methods, which is why we looked for a selection of methods that consider the plausibility of generated CEs. Two methods were, however, not tested for the following reasons:

- PlaCE [1] does not allow for an implementation for Neural Networks. It also cannot model categorical features well.

- DACE [29] does not have a public implementation that would allow for Neural Networks as models. It might also struggle with the size of datasets used here since they are an order of magnitude larger, and DACE computes the Local Outlier Factor, meaning that the formulation size increases linearly with the increase in the number of samples.